Materials Physics and Mechanics 42 (2019) 373-379 Received: May 30, 2019

MODEL FOR THE FORMATION OF GaAs-Au AXIAL NANOWIRE HETEROSTRUCTURES UNDER FLASH LAMP ANNEALING

Vladimir G. Dubrovskii*

ITMO University, Kronverkskiy pr. 49, 197101 St. Petersburg, Russia

*e-mail: dubrovskii@mail.ioffe.ru

Abstract. Semiconductor-metal nanowire heterostructures have attracted a particular interest over the last decade. However, they often suffer from low interface and crystalline quality. Here, we present a model for the formation of GaAs-Au axial nanowire heterostructures from GaAs/Au core-shell nanowires encapsulated into SiO_2 under flash lamp annealing, as described in the previous work. The model reveals the basic mechanism and establishes the main control parameters of the process which enable high quality GaAs-Au heterostructures. It can also be used for the optimization of similar processes in a wide range of material combinations.
Keywords: GaAs-Au nanowire heterostructures, SiO_2 template, flash lamp annealing, phase diagram, modeling

1. Introduction

High quality quasi 1D periodic structures of semiconducting and metallic layers are interesting from the fundamental viewpoint as well as for applications in spintronics, plasmonics and metal base transistors. In this respect, semiconductor nanowires (NWs) offer an ideal template [1,2]. These NWs show a number of advantages over planar layers and even quantum dots, in particular, regarding their dislocation-free growth in highly mismatched material systems [3,4] and organization in regular arrays [1,2]. NWs of III-V compound semiconductors can be grown via the vapor-liquid-solid [5,6] with either Au [7] or Ga [8] catalysts, by selective area epitaxy [9,10], or in the self-induced approach [11]. There has been a tremendous progress in the synthesis and studies of high quality III-V NW heterostructures [2]. However, fabrication of quasi 1D heterostructures, consisting of crystalline semiconductor material and metal, was very challenging in the past.

In Ref. [12], a general approach was presented for the formation of quasi 1D axial semiconductor-metal NW heterostructures with epitaxial relationship and sharp interfaces. The process was discussed for an important material system of GaAs-Au. Furthermore, the feasibility of the method for other material combinations was demonstrated. The method relied upon mature semiconductor processing techniques as described below, and enabled the reformation of GaAs/Au core-shell NWs encapsulated into SiO_2 into a sequence of axial GaAs-Au heterostructures under flash lamp annealing (FLA). In this work, we develop a model for this peculiar process, which reveals the basic mechanism and establishes the main control parameters leading to high quality axial GaAs-Au heterostructures.

2. Experimental procedure

Figure 1 illustrates the key technological steps applied in Ref. [12] for the formation of GaAs-Au NW heterostructures using standard semiconductor processing techniques and FLA. With these techniques, we were able to process wafer-scale samples and at the same time

http://dx.doi.org/10.18720/MPM.4242019_1
© 2019, Peter the Great St. Petersburg Polytechnic University
© 2019, Institute of Problems of Mechanical Engineering RAS

ensure the excellent control over the NW morphology. The starting point is an array of <111>-oriented GaAs NWs, grown on a Si substrate using the self-catalyzed vapor-liquid-solid molecular beam epitaxy [8], as shown in Fig. 1 (a). After removing the native oxide, the Au is introduced by sputtering deposition, resulting in the GaAs-Au core-shell NWs shown in Fig. 1 (b). Subsequently, the radial GaAs-Au NWs are encapsulated in a 20 nm thick silicon oxide shell using plasma enhanced chemical vapor deposition, as shown in Fig. 1 (c). The final axial semiconductor-metal NW heterostructures [Fig. 1 (d)] are formed by melting and reconfiguration of the NW core during a 20 ms FLA pulse with an energy density of 40 to 60 J/cm². The FLA energy as well as the preheating of the sample before FLA was carefully adjusted to ensure complete melting of the encapsulated GaAs-Au NW core. More details of the process and the corresponding experimental data are given in Ref. [12].

This processing technique reminds of the rapid melt growth (RMG) [13-15], first used by Liu et al. [15] for obtaining high quality Ge-on-insulator structures on Si substrates and then extended to other material systems including ternary InGaAs [15]. RMG method also uses SiO_2 microcrucibles to contain the Ge or InGaAs liquid during the crystallization anneal. The novelty of the approach described in Ref. [12] is in adding the noble Au metal to GaAs compound semiconductor and designing an optimized FLA procedure for fabrication of axial GaAs-Au heterostructures in quasi 1D NW geometry.

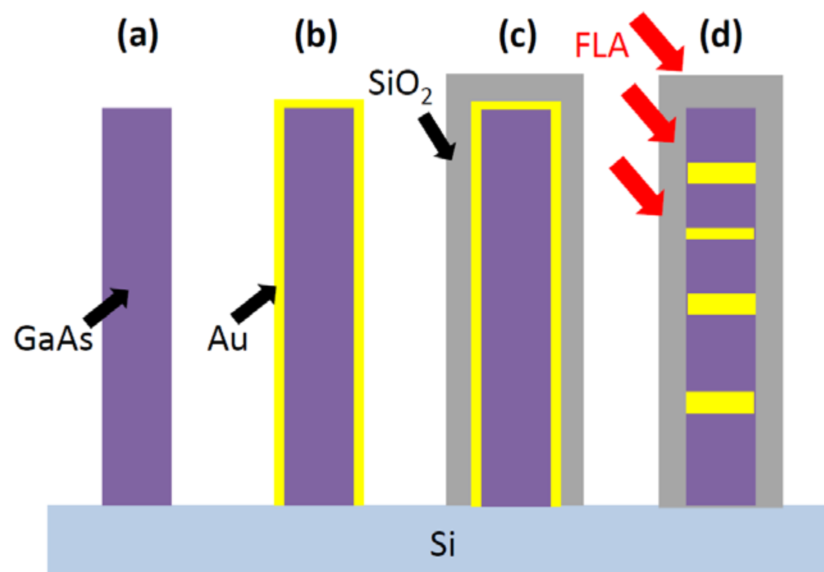

Fig. 1. Illustration of the key steps for fabrication of axial GaAs-Au heterostructures under FLA: (a) Epitaxial GaAs NWs on Si; (b) core-shell GaAs/Au NWs obtained after deposition of a thin Au layer onto the NWs; (c) encapsulation of the GaAs/Au core in the protective SiO_2 matrix; and (d) axial GaAs-Au heterostructures obtained after pre-heating and FLA by spatial rearrangement of Au in GaAs

3. Model

In modeling, we try to understand and quantify the peculiar mechanism of phase separation in GaAs-Au alloy, leading to rearrangement of the initial radial GaAs-Au heterostructure into a sequence of axial heterostructures, with rather sharp interfaces. As mentioned earlier, melting of the encapsulated GaAs-Au core under FLA with an optimized optical power should be the necessary for such a rearrangement. First, we notice that the melting temperature of GaAs is higher than that of Au [see the phase diagram in Figure 2 (a)] and hence melting of GaAs is expected to be the critical step. Using the parameters of GaAs [16] listed in Table 1, its

thermal diffusivity $k/(c\rho)$ can be estimated at $\sim 2.8\times 10^{13}$ nm^2/s (with k as the thermal conductivity, c as the specific heat capacity and ρ as the density). Therefore, temperature will equilibrate over the NW width in ~ 10^{-11} s for the typical NW radius R of 36 nm. This time is very short and hence we can consider a homogeneous temperature of the core T. The temperature changes in time due to FLA according to

$$\frac{dT}{dt}=\frac{2I_0(1-r)\alpha}{c\rho}\Theta(t-\tau)-\frac{2\sigma T^4}{c\rho R}. \quad (1)$$

Here, $\Theta(t-\tau)=1$ at $t\le\tau$ (under FLA) and 0 at $t>\tau$ (after FLA is turned off), $\tau=$ 20 ms is the duration of the FLA pulse, I_0 is the power density of FLA ($I_0\tau=$ 40 to 60 J/cm^2), r is the reflectivity of the core, including that of the Au layer, α is the effective light adsorption coefficient, and σ is the Stefan-Boltzmann constant The first term in Eq. (1) describes the temperature increase under FLA, while the second is the loss due to thermal (black body) radiation, as in Refs. [17,18]. Note that the first term in Eq. (1) is independent of R (at $\alpha R<<1$, which always holds for NWs of several tens of nanometers in width), while the second term scales inversely proportional to R [17,18].

Table 1. Parameters of GaAs used in calculations

k W/(m·K)	c J/(kg·K)	ρ kg/m^3	σ W/(m^2·K^4)	R nm	α cm^{-1}	r
52	350	5.32×10^3	5.67×10^{-8}	32	10^4	0.7

The time-dependent temperature of the core is obtained from Eq. (1) in the universal form

$$\frac{t}{t_*}=\frac{1}{4}\left[\ln\left(\frac{1+y}{1-y}\right)-\ln\left(\frac{1+y_0}{1-y_0}\right)\right]+2(\arctan y-\arctan y_0)\ \text{at}\ t\le\tau,$$

$$y=\frac{1}{\left[1+3(t-\tau)/t_*\right]^{1/3}}\ \text{at}\ t>\tau, \quad (2)$$

with $y=T/T_{\max}$. This dependence is controlled by the two parameters, the maximum temperature $T_{\max}$ and the characteristic time t_*, which determines the rate of the temperature increase (or decrease) under FLA and without FLA. These parameters are given by

$$T_{\max}=\left[\frac{I_0(1-r)\alpha R}{\sigma}\right]^{1/4},\quad t_*=\frac{c\rho R}{2\sigma T_{\max}^3}, \quad (3)$$

and quantify the time dependence of the core temperature for a given material combination.

4. Results and discussion

With the parameters of GaAs listed in Table 1, we obtain $T_{\max}=1350$ K, $t_*=0.217$ ms at $I_0\tau=40$ J/cm^2 and $T_{\max}=1500$ K, $t_*=0.159$ ms at $I_0\tau=60$ J/cm^2. Time evolution of temperatures for these parameters is shown in Fig. 2 (b), in the case without pre-heating. Very importantly, the characteristic times required to reach the maximum temperature under FLA and to decrease it without FLA appear very short, mush shorter than the duration of PLA pulse. The return to room temperature is however noticeably longer than the temperature increase under FLA.

Let us now see how this temperature behavior affects the state of the core. As the GaAs-Au core is fully encapsulated in SiO_2, the composition of a GaAs-Au alloy is fixed

throughout the entire FLA process. Our GaAs remains stoichiometric even in the liquid phase, because the desorption of As is blocked by solid SiO_2 shell. This property considerably simplifies the compositional analysis compared to the case of vapor-liquid-solid III-V NWs [19-21], where highly volatile group V species easily desorb and hence their concentration in a catalyst droplet changes drastically depending on the growth conditions. Here, we can use the pseudo-binary phase diagram of the GaAs-Au alloy [1] with stoichiometric GaAs in both liquid and solid states, as shown in Fig. 2 (a). At least in the GaAs-rich region of the diagram, the solid state is immiscible, that is, consists of a mixture of pure GaAs and Au crystallites. Above the eutectic temperature of 903 K, the alloy consists of GaAs-Au liquid and pure GaAs crystallites, with temperature-dependent fractions of liquid and the remaining solid GaAs. Above the liquidus, the GaAs-Au alloy becomes a single liquid melt, encapsulated in SiO_2 shell (which remains solid below 1980 K).

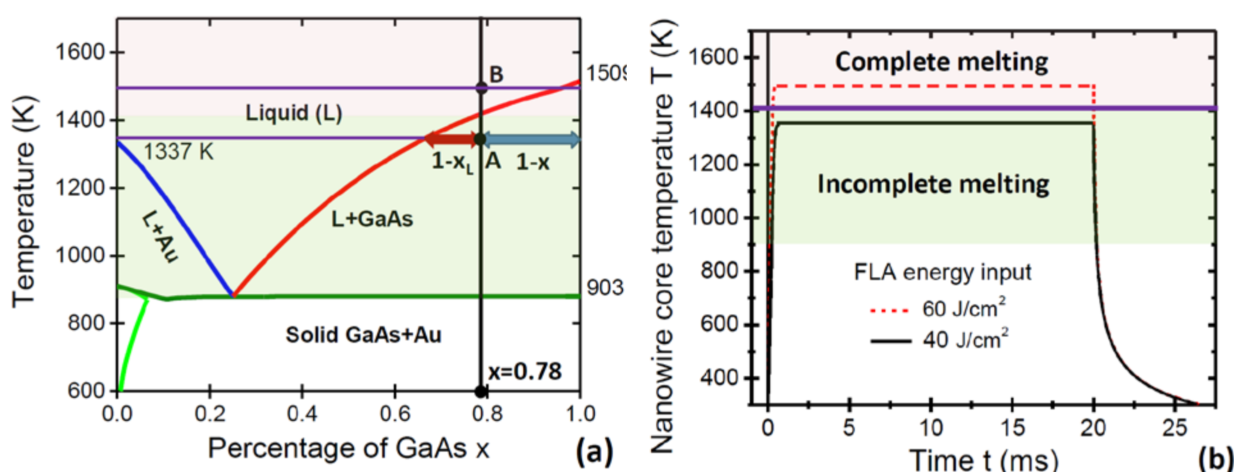

Fig. 2. (a) Pseudo-binary phase diagram of GaAs-Au alloy [1], with an almost horizontal solidus at 903 K, and the liquidus separating a mixture of GaAs-Au liquid with solid GaAs at lower temperatures from a single melt at higher temperatures (b)

Time dependence of the NW core temperature under 20 ms FLA pulse with 40 J/cm^2 (solid line) and 60 J/cm^2 (dashed line) energy input. The shaded regions in (a) and (b) indicate the states of incomplete (from 903 K to ~ 1410 K) and complete (above ~ 1410 K) melting of GaAs-Au alloy at a fixed GaAs fraction of 0.78, estimated from the NW geometry [12]. It is seen that 40 J/cm^2 FLA leads to a maximum core temperature of 1350 K, corresponding to the incomplete melting, while increasing the FLA power to 60 J/cm^2 yields a temperature of 1500 K, where the alloy is completely molten. Vertical line in (a) shows heating of the core with a fixed $x = 0.78$ to point A at 1350 K under 40 J/cm^2 FLA and to point B under 60 J/cm^2 FLA. Horizontal line crossing point A shows the tie line. At 1350 K, the GaAs content in liquid GaAs-Au alloy is x_L and the fraction of liquid is $(1-x)/(1-x_L)$, while the fraction of remaining solid GaAs is $(x-x_L)/(1-x_L)$. These diagrams quantitatively explain the experimental data presented given in Ref. [12], namely, the presence of Au clusters blocked by solid GaAs under 40 J/cm^2 FLA, and the regular sequence of GaAs-Au axial heterostructures under 60 J/cm^2 FLA.

It is easy to estimate the fraction of GaAs x in GaAs-Au NWs of Ref. [12] from their initial core-shell geometry. Using $N_{Au} / N_{GaAs} = 2h_{Au}\Omega_{GaAs} / (R\Omega_{Au})$, with $h_{Au} = 2$ nm as the thickness of the Au layer, $R = 36$ nm, $\Omega_{GaAs} = 0.0452$ nm^3 as the elementary volume of solid

GaAs and $\Omega_{Au} = 0.0170$ nm^3 of solid Au [2], we obtain $x = N_{GaAs}/(N_{GaAs} + N_{Au}) \cong 0.78$. This determines the position of vertical line in Fig. 2 (a), corresponding to heating of GaAs-Au alloy at this fixed composition. Heating the system up to point A under 40 J/cm^2 [corresponding to a temperature of 1350 K according to Fig. 2 (b)] renders the system into the regime of incomplete melting. According to the lever rule [22], the fraction of liquid equals $(1-x)/(1-x_L)$, while the fraction of solid GaAs equals $(x-x_L)/(1-x_L)$, with x_L as the GaAs content in liquid. The remaining solid GaAs suppresses the diffusion of Au through the volume of the core, which explains the presence of Au clusters as discussed in Ref. [12]. By increasing the FLA power density from 40 J/cm^2 to 60 J/cm^2, we are able to cross the liquidus, which is why the alloy at 1500 K [point B in Fig. 2 (a)] is completely molten. This yields free diffusion of Au through the entire volume of encapsulated liquid, resulting in a more regular sequence of axial GaAs-Au heterostructures, as observed in Ref. [12].

As regards the final stage of heterostructure formation, it occurs after stopping the FLA irradiation, where the liquid (or partially liquid) NW core rapidly cools down and becomes solid again. The width and the number of GaAs-Au heterostructures is determined by complex kinetic processes at this stage. These processes require a separate study. We note, however, that immiscibility of the GaAs-Au solid alloy should help to achieve atomically sharp heterointerfaces, as predicted in Ref. [20] for a different system (axial NW heterostructures in immiscible InAs-GaAs alloy). Overall, our model establishes the basic mechanism for the rearrangement of encapsulated semiconductor-metal NWs (actually, of whatever initial form) into axial heterostructures under heating. It shows why the FLA power should be carefully optimized to yield the complete melting of the alloy, and confirms the importance of encapsulation of the alloy within the solid SiO_2 shell. Melting of the core may be achieved by applying other heating techniques, and the whole procedure is expected to work equally well for a wide range of semiconductor-metal material systems. It will also be interesting to consider horizontal NW geometries such as described in Ref. [23].

In conclusion, the developed model explains the governing mechanism of the formation of axial GaAs-Au heterostructures by the complete melting of the GaAs-Au alloy enclosed in the solid SiO_2 matrix under FLA. The parameters of the process, such as the FLA pulse duration and energy credit, should be optimized to yield the molten GaAs-Au alloy in solid SiO_2 for a given composition. The model can be used to quantify and optimize similar processes in a wide range of material systems. Overall, this method looks very promising for fabrication of high quality semiconductor-metal NW heterostructures.

Acknowledgement. *The author gratefully acknowledges financial support of the Russian Science Foundation under the grant 19-72-30004.*

References

[1] Zhang A, Zheng G, Lieber CM. *Nanowires: Building blocks for nanoscience and nanotechnology*. Switzerland: Springer; 2016.

[2] Dubrovskii VG. Theory of VLS growth of compound semiconductors. In: Morral AF, Dayeh SA, Jagadish C. (eds). *Semiconductors and Semimetals*. *Vol. 93*. Burlington: Academic Press; 2015. p.1-78.

[3] Ng KW, Ko WS, Tran TTD, Chen R, Nazarenko MV, Lu F, Dubrovskii VG, Kamp M, Forchel A, Chang-Hasnain CJ. Unconventional Growth Mechanism for Monolithic Integration of III–V on Silicon. *ACS Nano*. 2013;7(1): 100-107.

[4] Cirlin GE, Dubrovskii VG, Petrov VN, Polyakov NK, Korneeva NP, Demidov VN, Golubok AO, Masalov SA, Kurochkin DV, Gorbenko OM, Komyak NI, Ustinov VM, Egorov AY, Kovsh AR, Maximov MV, Tsatusul'nikov AF, Volovik BV, Zhukov AE, Kop'ev PS,

Alferov ZhI, Ledentsov NN, Grundmann M, Bimberg D. Formation of InAs quantum dots on a silicon (100) surface. *Semiconductor Science & Technology.*1998;13(11): 1262-1265.
[5] Wagner RS, Ellis WC. Vapor liquid solid mechanism of single crystal growth. *Applied Physics Letters*. 1964;4: 89-90.
[6] Dubrovskii VG, Sibirev NV, Cirlin GE. Kinetic model of the growth of nanodimensional whiskers by the vapor-liquid-crystal mechanism. *Technical Physics Letters*. 2004;30(8): 682-686.
[7] Dubrovskii VG, Soshnikov IP, Cirlin GE, Tonkikh AA, Samsonenko YB, Sibirev NV, Ustinov VM. On the non-monotonic lateral size dependence of the height of GaAs nanowhiskers grown by molecular beam epitaxy at high temperature. *Physica Status Solidi B*. 2004;241(7): R30-R33.
[8] Matteini F, Dubrovskii VG, Rüffer D, Tütüncüoğlu G, Fontana Y, Morral AF. Tailoring the diameter and density of self-catalyzed GaAs nanowires on silicon. *Nanotechnology.* 2015;26(10): 105603.
[9] Mohan P, Motohisa J, Fukui T. Controlled growth of highly uniform, axial/radial direction-defined, individually addressable InP nanowire arrays. *Nanotechnology.* 2004;16(12): 2903.
[10] Gao Q, Dubrovskii VG, Caroff P, Wong-Leung J, Li L, Guo Y, Fu L, Tan HH, Jagadish C. Simultaneous selective-area and vapor–liquid–solid growth of InP nanowire arrays. *Nano Letters*. 2016;16(7): 4361-4367.
[11] Dubrovskii VG, Consonni V, Trampert A, Geelhaar L, Riechert H. Scaling thermodynamic model for the self-induced nucleation of GaN nanowires. *Physical Review B*. 2012;85(16): 165317.
[12] Benter S, Dubrovskii VG, Bartmann M, Campo A, Zardo I, Sistani M, Stöger-Pollach M, Lancaster S, Detz H, Lugstein A. Quasi One-Dimensional Metal–Semiconductor Heterostructures. *Nano Letters.* 2019;19(6): 3892-3897.
[13] Liu Y, Deal MD, Plummer JD. High-quality single-crystal Ge on insulator by liquid-phase epitaxy on Si substrates. *Applied Physics Letters*. 2004;84(14): 2563.
[14] Liu Y, Deal MD, Plummer JD. Rapid melt growth of germanium crystals with self-aligned microcrucibles on Si substrates. *Journal of Electrochemical Society*. 2005;152(8): G688-G693.
[15] Bai X, Chen CY, Mukherjee N, Griffin PB, Plummer JD. Rapid melt growth of single crystal InGaAs on Si substrates. *Advances in Materials Science and Engineering*. 2016:2016; 7139085.
[16] Levinshtein ME, Rumyantsev SL. Gallium Arsenide (GaAs). In: *Handbook series on semiconductor parameters. Vol. 1*. Levinshtein M, Rumyantsev SL, Shur M. (eds.) Singapore: World Scientific; 1996. p.77-103.
[17] Glas F, Harmand JC. Calculation of the temperature profile in nanowhiskers growing on a hot substrate. *Physical Review B*. 2006;73(15): 155320.
[18] Sibirev NV, Soshnikov IP, Dubrovskii VG, Arshansky E. Temperature profile along a nanowhisker growing in high vacuum. *Technical Physics Letters*. 2006;32(4): 292-295.
[19] Glas F. Chemical potentials for Au-assisted vapor-liquid-solid growth of III-V nanowires. *Journal of Applied Physics*. 2010;108: 073506.
[20] Dubrovskii VG, Koryakin AA, Sibirev NV. Understanding the composition of ternary III-V nanowires and axial nanowire heterostructures in nucleation-limited regime. *Materials & Design*. 2017;132: 400-408.
[21] Dubrovskii VG, Grecenkov J. Zeldovich nucleation rate, self-consistency renormalization, and crystal phase of Au-catalyzed GaAs nanowires. *Crystal Growth & Design*. 2015;15(1): 340-347.

[22] Smith WF, Hashemi J. *Foundations of materials science and engineering*. 4th ed. McGraw-Hill; 2006.
[23] Friedl M, Cerveny K, Weigele P, Tütüncüoglu G, Marti-Sanchez S, Huang C, Patlatiuk T, Potts H, Sun Z, Hill MO, Güniat L, Kim W, Zamani M, Dubrovskii VG, Arbiol J, Lauhon LJ, Zumbühl DM, Morral AF. Template-assisted scalable nanowire networks. *Nano Letters*. 2018;18(4): 2666-2671.